Chronopotentiometry of Titania Film Electrodes in Aqueous Media

Wenjian Sun, C. R. Chenthamarakshan, and Krishnan Rajeshwar*

Department of Chemistry and Biochemistry, The University of Texas at Arlington, Arlington, Texas 76019-0065

Received: April 9, 2002; In Final Form: August 7, 2002

Temporal changes in the potential of TiO_2 films (supported on Au substrates) were monitored under ultraviolet irradiation in aqueous media. Prior to these experiments, mimicing heterogeneous photocatalysis reaction conditions, the open-circuit potentials (E_{oc}) of the prepared TiO_2 films were monitored as a function of medium pH in the 3−11 range. A slope of −26 mV/pH was measured; this value is compared with previous studies of the pH dependence of E_{oc} and the TiO_2 flat-band potential, E_{fb}. Perhaps the most remarkable aspect of the presented (E_{ph}−t) profiles concerns the very slow (minute regime) changes in the TiO_2 film potential when the UV light is turned on. The extent of negative potential excursion (when the UV light is initially switched on) and the plateau potential attained (at times greater than ∼5 min) are dependent on the nature of the metal ion "depolarizer", the incident photon flux, and the presence of any co-additive in the 0.05 M Na_2SO_4 supporting electrolyte. When the light is turned off, the TiO_2 film potential returns to its rest value (in the "dark") in exponential fashion. A simple model, based on initial photocharging of the TiO_2 film/solution interface and subsequent carrier trapping/detrapping events, is presented to account for the observed trends in the measured (E_{ph}−t) profiles. Simulations based on this model afford chronopotentiometric profiles in good agreement with their experimental counterparts.

Introduction

Anodic photoprocesses have been exceedingly well studied on titania electrode surfaces and in aqueous suspensions in recent years.[1−4] Much of the impetus for these studies undoubtedly stems from the fact that a wide range of organic compounds (many of them, environmental pollutants) can be oxidized by the photogenerated hydroxyl radicals or holes on the titania surface. Contrastingly, cathodic photoprocesses involving TiO_2 and reducible solution species have received much less scrutiny. Optimization of the photocatalytic oxidation pathway requires accelerating the cathodic conjugate half-reaction as well,[5] and the importance of catalyzing the dioxygen reduction step in this regard has been underlined in previous studies.[6,7]

Our laboratory has recently focused on the photocatalytic reactivity of metal ions on TiO_2 surfaces.[8−18] The indirect reduction of metal ions with rather negative standard reduction potentials (Figure 1), which is mediated by free radicals generated by the initial photooxidation of organic "anchor" species such as formate, has been of particular interest in these studies.[9−11,15,16] In the spirit of extending the available range of measurement probes on photocatalytic reaction mechanisms (with particular emphasis on cathodic photoprocesses), we describe below our use of chronopotentiometry for the study of TiO_2 film electrodes in aqueous media under UV irradiation.

We use the term "chronopotentiometry" (CP) in the present context to be descriptive of measurements of the potential of the working electrode (TiO_2 film in our case) versus a reference electrode, as a function of time, under UV irradiation. Thus the small constant current that is normally employed in CP measurements[19] is instead set in our case, by the (constant) incident photon flux.[20] We show below that TiO_2 films manifest photopotential (E_{ph}) temporal changes that are surprisingly slow (in the minute regime) and the (E_{ph}−t) profiles are sensitive to the photocatalytic reactivity of the metal ions on the UV-irradiated TiO_2 surface. We additionally find that a simple model and simulations based on photocharging of the TiO_2/electrolyte interface upon UV excitation followed by carrier trapping events, provide a good explanation for the observed trends in the (E_{ph}−t) profiles.

Few studies exist, at least to our knowledge, where (E_{ph}−t) profiles of TiO_2 photocatalysts have been monitored. Coulostatic-flash irradiation of n-TiO_2 single-crystal electrodes in aqueous KNO_3 supporting electrolyte with a pulsed laser source afforded time-resolved measurements of photopotential transients in the submicrosecond time domain.[21] A gold-plated platinum wire was used as a measurement probe (versus Ag/AgCl, saturated KCl reference) to monitor potential changes when platinized anatase particles in NaOH were subjected to pulsed illumination from a 500 W xenon lamp.[22] The observed potential changes spanned the minute time domain in this case. The overlapping aspects from these earlier studies will be further discussed in what follows.

Experimental Section

Chemicals. Zinc sulfate (Aldrich, 99%), cadmium sulfate (Aldrich, 98%), thallium sulfate (Johnson Matthey, 99.9%), lead nitrate (Alfa Aesar, 99.999%), and manganese sulfate (Fisher, 99.2%) were used without further purification. Copper sulfate (Baker, 99.9%), potassium dichromate (Mallinckrodt, 99.9%), sodium formate (Alfa Aesar, 99%), methanol (Sigma, 99+%), sodium oxalate (Sigma, 99.5%), and sodium acetate (Aldrich, 99%) were used without further purification. The TiO_2 (Degussa P-25) used was predominantly anatase and had a specific surface area of ∼60 m^2/g. Deionized water (18 MΩ) was used in all cases for making solutions or suspensions (unless otherwise specified).

* To whom correspondence should be addressed. E-mail: rajeshwar@uta.edu.

10.1021/jp020935x CCC: $22.00
Published on Web 10/15/2002

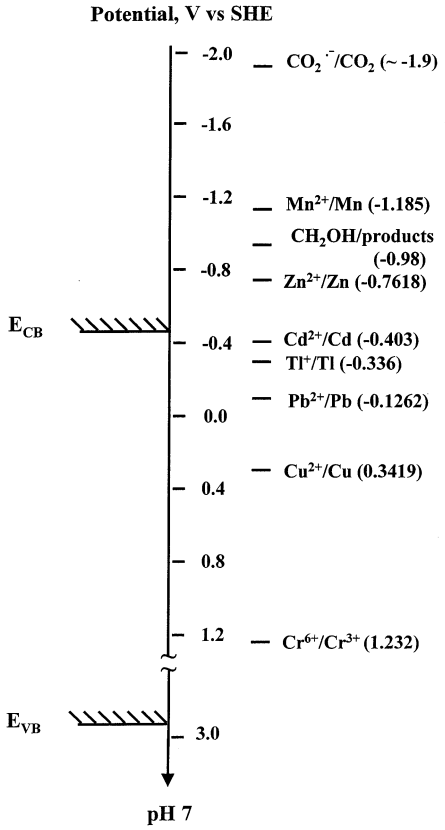

Figure 1. Relative position of the conduction and valence band-edges in TiO_2 (at pH 7) and the redox energy levels (standard reduction potentials) for the seven metal ions of interest in this study and for the radicals derived from the carboxylate anions and methanol (Note the discontinuity in the potential scale at ~1.6 V).

TiO_2 Film Electrode Preparation. A TiO_2 suspension (10 g/L) was made by mixing 0.25 g of TiO_2 powder with 25 mL of 2-propanol in a 100 mL beaker. Gold foils (22 mm × 5 mm, 0.25 mm thickness, Alfa Aesar, 99.95%) were used as substrates, one side of which was masked with cellophane tape to selectively deposit TiO_2 only on the other side of the foil. The TiO_2 suspension was stirred for 3 h prior to dipping of the gold foils. This was done to ensure a high dispersion of the TiO_2 particles in the suspension. The coated substrates were promptly withdrawn after immersion in the suspension for 2 s. After air-drying for 5 min., the films were heated in air at 300 °C for 10 min. This dip−coat−anneal procedure was repeated eight times until a thick uniform, white film was obtained. Finally, the TiO_2/Au films were heated in a muffle furnace (Model M15A-2A, Blue M Electric Co., Blue Island, IL) for 17 h at 300 °C. The films thus prepared had a nominal thickness of 7.5 ± 2.0 μm, as measured on an Alfa-Step 200 profilometer (Tencor Instruments, Mountain View, CA).

Considerable effort was devoted to ensuring reproducible performance of the TiO_2 film electrodes. To this end, a series of optimization trials were carried out using the number of dip−coat−anneal cycles, the anneal temperature, and the anneal time as variables. The combination described above was found to yield the most satisfactory performance in the CP experiments. Figure 2 contains sample ($E-t$) profiles from four different electrodes illustrating the variability that was typical after the optimization exercise. These sample-to-sample variations were considered negligible relative to the changes that were observed in the ($E-t$) profiles to be described below.

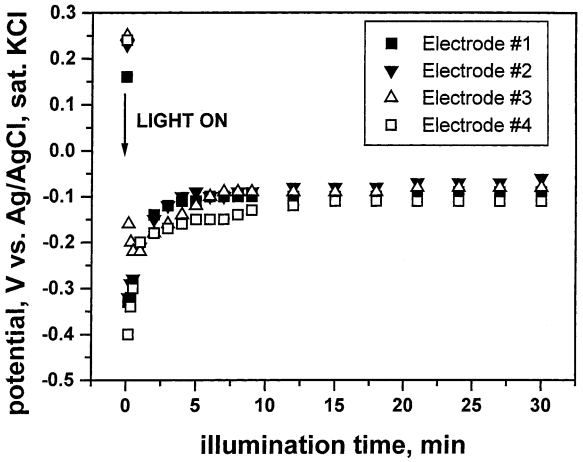

Figure 2. Sample ($E_{ph}-t$) profiles for four different TiO_2 films in 0.05 M Na_2SO_4 electrolyte. The films were irradiated as described in the Experimental Section. The CP data are shown as discrete data points for better clarity.

Instrumentation and Procedures. In all the cases, the TiO_2 film electrode was first equilibrated with a given aqueous medium for 1 h in the dark. The supporting electrolyte was 0.05 M Na_2SO_4 (except in the Pb^{2+} ion case for solubility reasons when 0.05 M NaCl was used instead) and the solution additionally contained either the metal ion (200 μM) and/or any co-additive, as needed. The solutions were continually purged with ultrapure N_2 both during the dark equilibration period and during UV illumination of the TiO_2 film surface. Because of this agitation, mass transport limitations are not considered to exert any influence on the ($E-t$) profiles to be discussed below.

The UV light source was a 75 W xenon arc lamp (Oriel, Stratford, CT). This source was placed 15 cm away from the TiO_2/Au working electrode surface. The backside (Au side) insulation also served to mask it from the light source to preclude scattered light from reaching it. The working electrode and a Ag/AgCl, saturated KCl reference electrode (Bioanalytical Systems, W. Lafayette, IN) were reproducibly positioned inside a 100 mL quartz beaker. The open-circuit and photopotentials (E_{oc} and E_{ph}, respectively) were measured on a Model CV-27 Bioanalytical Systems Voltammograph instrument, and the ($E-t$) profiles were displayed on a Houston Instrument Model 2000 recorder.

In experiments where the medium pH was intentionally varied, sulfuric acid or sodium hydroxide (both at 0.1 M) were used to adjust the solution values in the range from pH 3 to 11. Unless otherwise mentioned, the other CP experiments were performed at a "natural" value of the pH in the 6−7 range. The nominal incident photon flux was 2.2 mW/cm^2, as measured with an Oriel Model 70260 Radiant Power/Energy meter. This flux was varied in a series of CP experiments by inserting variable numbers of metal mesh screens that were calibrated to provide known fractions of the above photon flux. All measurements were performed at the laboratory ambient temperature (25 ± 5 °C).

Results

Dependence of E_{oc} for TiO_2/Au Electrodes on pH of the Medium. Figure 3 contains data, pooled from nine experiments, on how E_{oc} varies with solution pH in the range from 3 to 11. These data are all for 0.05 M Na_2SO_4 supporting electrolyte, where the pH was adjusted to the desired value (see Experimental Section). The data for the correlation in Figure 3 included those from one set of experiments where the same TiO_2

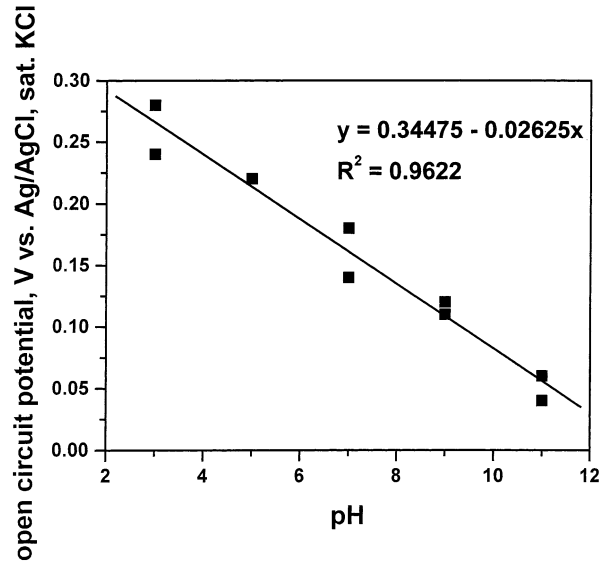

Figure 3. Dependence of E_{oc} on the pH of the medium (working electrode: TiO_2 films, 0.05 M Na_2SO_4 electrolyte). The solid line is a least-squares fit.

electrode was exposed to media of various pH values as well as those from another set that utilized a different TiO_2 film for each medium pH. The correlation coefficient was 0.98 for the least-squares fit in Figure 3. E_{oc} obviously shifts in the negative direction with increasing pH by ~26 mV/pH unit. A comparison of this trend with those observed previously by other authors, is deferred to a latter juncture.

Comparison of ($E-t$) Profiles for Control and in the Presence of Various Metal Ions. In these experiments, after the dark equilibration period (see Experimental Section), the UV excitation light was turned on, and the ($E_{ph}-t$) profiles were monitored for the TiO_2 working electrode. The control run omitted the metal ion in the supporting electrolyte.[23] In all other cases, the metal ion was present at the 200 μM level. As discussed by us recently,[18] the metal ions can be broadly divided into three categories on the basis of their photocatalytic reactivity with TiO_2.

Referring back to Figure 1, those species with rather negative standard reduction potentials ($E°$) (Mn^{2+}, Zn^{2+}, Cd^{2+})[24] are photocatalytically inert in that the TiO_2 conduction band (or subsequently trapped, see below) electrons have insufficient (or barely sufficient, in the Cd^{2+} case) energy to reduce them.[18] Thallium and Pb^{2+} ions with more positive $E°$ values are mildly reactive, and Cr^{6+} with a very positive $E°$ value is very reactive (Figure 1). The Cu^{2+} ion case represents an intermediate case, i.e., a "bridge" between the reactive and unreactive categories.[18]

As Figure 4 illustrates, distinctly different ($E_{ph}-t$) profiles are observed for the metal ions in these three categories. The control run mimics the profile observed for the unreactive metal ions (Mn^{2+}, Zn^{2+}, Cd^{2+}). Thus when the light is turned on, the potential in each case jumps in the negative direction (from the rest location) and then relaxes back to a more positive value that is maintained thereafter, all of the ($E_{ph}-t$) changes occurring within ~5 min after the light is switched on. We designate this stable potential attained as the plateau value.

The extent of negative excursion and the plateau value attained thereafter systematically vary in progressing from the unreactive → moderately reactive (Tl^+, Pb^{2+}) → very reactive (Cr^{6+}) cases, the extent of negative excursion being progressively less (or even virtually nonexistent as in the Cr^{6+} case) and the plateau potential being increasingly more positive.

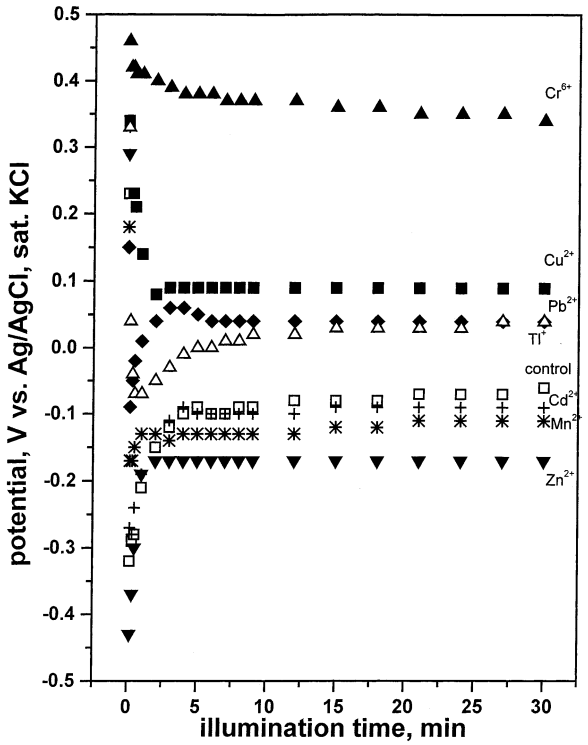

Figure 4. CP data for the seven metal ions and for a control run (see text, other conditions as in Figure 2).

Chronopotentiometric Behavior in the Presence of Co-Additives. Co-additives in a photocatalysis medium can exert an effect in terms of either inducing adsorption of the metal ion on the TiO_2 surface or generating free radicals (via their initial oxidation by the photogenerated holes in TiO_2). The free radicals are highly reducing and are subsequently capable of reducing the metal ion via a galvanic (electron transfer) process (see also Figure 1).[9-11,15,16] Alternately, the co-additive can minimize electron−hole pair recombination in TiO_2 and accelerate the reduction pathway by improving the kinetics of the conjugate photooxidation.[5] Carboxylate anions (formate, acetate, oxalate) and alcohols (methanol) were chosen as model co-additives for this study to explore these variant effects on the ($E-t$) profiles.

Figure 5 contains ($E_{ph}-t$) profiles for experiments where the metal ion was omitted; data for the four co-additives as well as for the control ion are compared. Contrasting with the trend in Figure 4 above and for the control run, no or little "upturn" in the ($E_{ph}-t$) profiles were observed after the initial negative excursion for the four co-additives. Both the extent of negative excursion and the magnitude of the negative plateau potential are ordered formate > oxalate ≫ acetate, methanol, with formate inducing the most negative values of E_{ph}.

Interestingly, addition of metal ions perturbed the ($E_{ph}-t$) profile only little, especially when a co-additive such as formate was present in the photocatalysis medium. This is exemplified by the data in Figure 6 for five metal ions. The profiles in Figure 6 are to be compared with their counterparts in Figures 4 and 5, respectively. Note that with formate present, the E_{ph} values are pinned to negative values after the light is turned on for both the unreactive (Mn^{2+}, Zn^{2+}) and mildly reactive (Tl^+, Pb^{2+}) metal ions (Figure 6). On the other hand, the very gradual decay of E_{ph} with time for Cr^{6+} is slightly "quenched" when formate is present, although the plateau potential is little affected by the co-additive (cf., Figures 4 and 6). In other words, the effect of metal ions appears to be "buffered" by the formate.

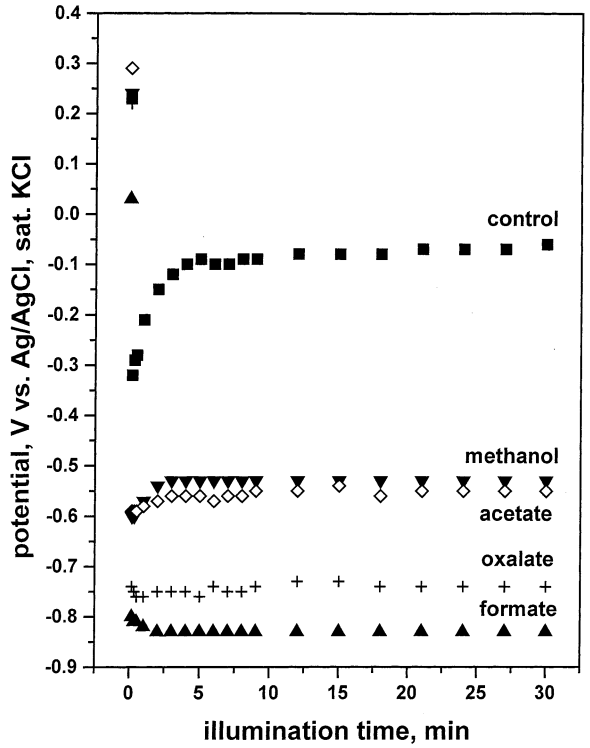

Figure 5. As in Figure 4 but only for the four co-additives and no metal ions in the solution. Control run shown for comparison. Other conditions as in Figure 2.

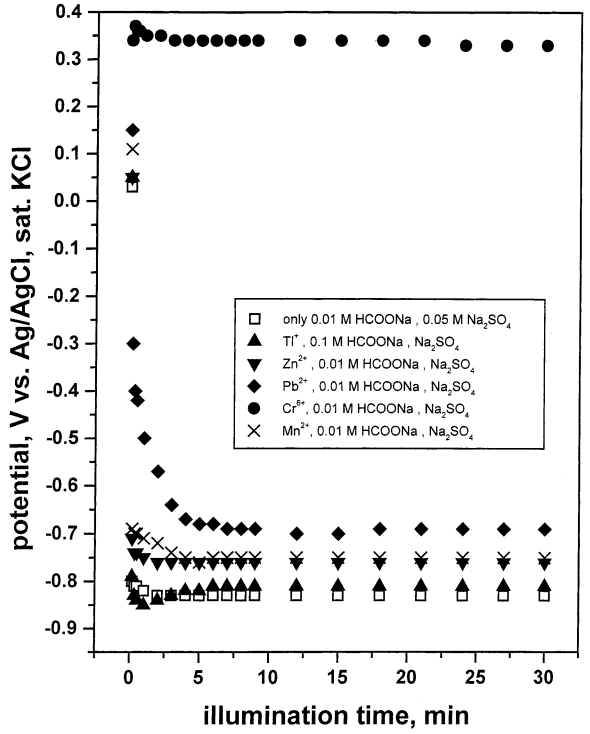

Figure 6. As in Figure 4 but for five metal ions additionally present along with the formate co-additive. The CP profile for formate + supporting electrolyte is reproduced from Figure 5 for comparison. Other conditions as in Figure 2.

Influence of Medium pH on the ($E-t$) Profiles. We have shown previously that the pH of the medium plays a crucial role in the TiO_2-assisted photocatalytic reduction of Cr^{6+} species.[13] Specifically, the reduction of hexavalent chromium (to the trivalent state) requires a healthy dose of proton supply

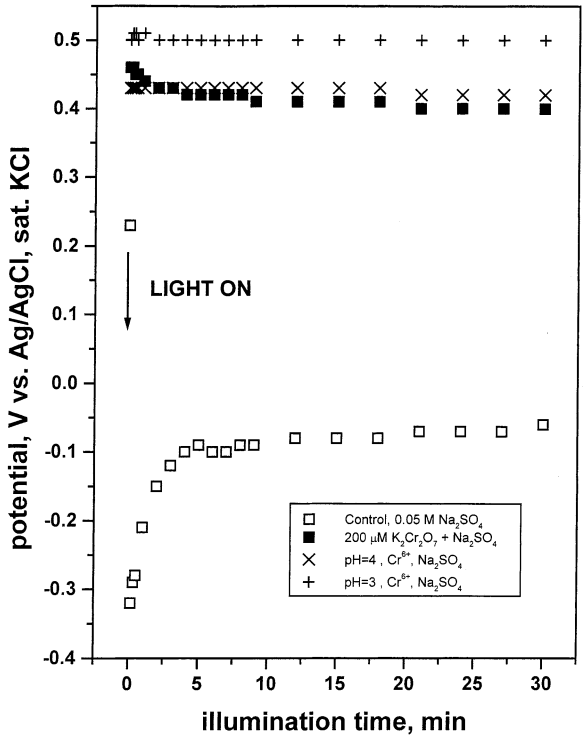

Figure 7. Influence of medium pH on the CP profiles for Cr^{6+}. The control run (at pH 7) is reproduced for comparison. Other conditions as in Figure 2.

to the TiO_2 particle/solution interface because protons are co-reactants in the $Cr^{6+} \rightarrow Cr^{3+}$ reduction process.[13]

All the experiments in Figures 2 and 4−6 were performed at the "natural" pH of the medium (close to pH 7). Figure 7 contains ($E_{ph}-t$) profiles for two cases where the pH was adjusted to acidic values (3 and 4, respectively). For comparison, the pH 7 data (from Figure 4) are also included. A shift in the potential to positive values is seen when the pH is lowered.

Influence of the Photon Flux and Turning Off the UV Light on the ($E-t$) Profiles. Figure 8 contains data illustrating how the incident photon flux (on the TiO_2 film surface) affects both the extent of the initial negative excursion of E_{ph} and the subsequent plateau potential attained. Thus both become increasingly more positive as the photon flux is progressively decreased. Figure 9 shows that the extent of negative shift of the potential (from the dark value) is linearly dependent on the incident photon flux.

When the UV excitation light is turned off, the potential steadily returns to the original (rest) value in an exponential fashion (data not shown). Consequently, in this time regime, a semilog plot of $\ln[E(t)/E_0]$ vs time is linear, as shown for four photon fluxes in Figure 10. The slopes of these plots (i.e., time constants) are seen to remain reasonably constant ($-0.006\,33 \pm 0.000\,28\ s^{-1}$) with varying photon flux (see insert, Figure 10).

Discussion

Dependence of E_{oc} on pH of the Medium. According to the triple-layer model[25,26] and the known behavior of oxide surfaces,[27,28] the potential-determining species are H_3O^+ and OH^-. As the pH of the medium increases, $Ti-O^-$ surface groups become preponderant relative to the $Ti-OH_2^+$ counterparts. Thus, flat-band potential (E_{fb}) measurements on both TiO_2 single crystals[29] and nanocrystalline[30] films have revealed a Nernstian pH dependence of E_{fb} (-0.059 V/pH). Other photochemical

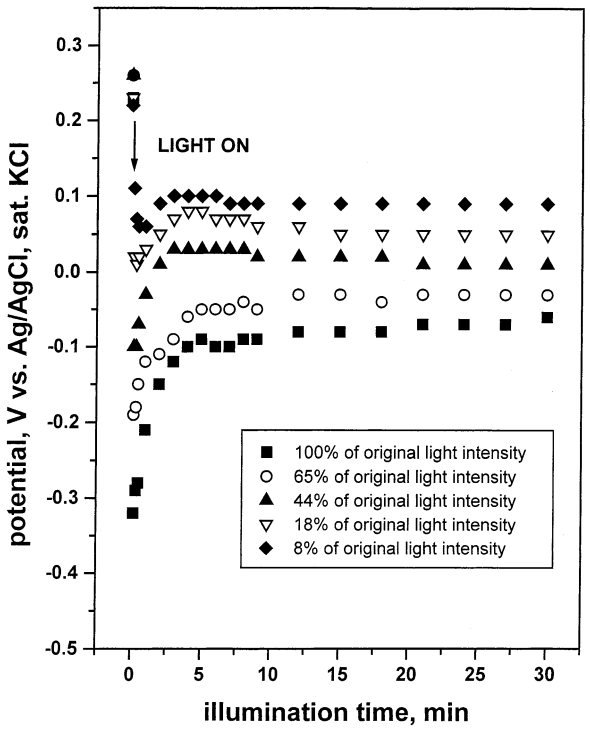

Figure 8. Influence of varying photon flux on the CP profiles in 0.05 M Na_2SO_4 supporting electrolyte. Other conditions as in Figure 2.

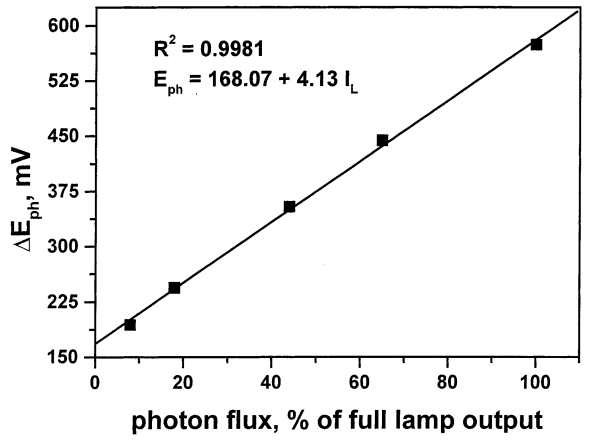

Figure 9. Plot of the magnitude of the light-induced potential shift (ΔE_{ph}) versus the incident photon flux. ΔE_{ph} values were culled from the data in Figure 8 and are for 10 s irradiation. The solid line is a least-squares fit of the data points.

measurements including colloidal TiO_2 particles and electron acceptors such as methyl viologen, have also been interpreted on the basis of such a shift in the TiO_2 conduction band edge with pH.[31,32] On the other hand, more recent E_{oc} measurements of Ti/TiO_2 electrodes prepared by thermal or electrochemical oxidation of titanium metal have revealed slopes of -0.039 ± 0.005 V in the range of pH 5−10.[33] Our new measurements of E_{oc} for nanocrystalline TiO_2 films (supported on Au) (Figure 3) are in reasonable agreement with this latter slope. The reason for the discrepancy between the observed E_{oc} vs pH and E_{fb} vs pH trends, even for nanocrystalline TiO_2 films, is still unclear. Complicating comparison of data generated in different laboratories is difficult due to the possible sensitivity of parameters such as E_{oc} and E_{fb} to surface material topography and/or preparation history. Disregarding quantitative differences, an overall trend of a negative shift in E_{oc} (or E_{fb}) with increasing pH, is evident.

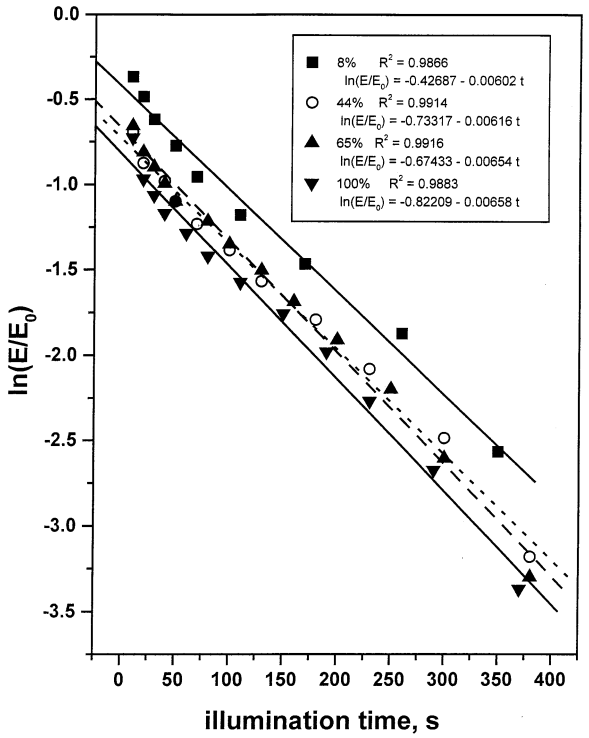

Figure 10. Semilog plots of the potential changes when the UV excitation light is turned off. The data (for four photon fluxes) illustrate the exponential dependence of potential on time. The solid lines are least-squares fits of the data points.

($E-t$) Profiles under UV Irradiation. Band gap excitation of TiO_2 creates electron−hole pairs. A number of these undergo recombination in the bulk, which is an extremely fast process.[34−37] The remainder diffuses to the semiconductor surface. A number of studies show evidence[38−48] that both electrons and holes in TiO_2 particles are trapped in surface sites. In the absence of suitable electron acceptors (donors), the trapped electrons (holes) undergo surface recombination. The final (steady-state) potential attained by the TiO_2 film under irradiation then reflects the competition between the carrier generation and recombination events. The initial negative excursion in E_{ph} when the light is turned on (Figures 2 and 4) can thus be rationalized in terms of the population of the conduction band with the photogenerated electrons. Considering that the Degussa P-25 TiO_2 particles used here are not intentionally doped, it is reasonable to assume that the "dark" Fermi level lies approximately at mid-gap. UV irradiation subsequently shifts it "up" or in the negative direction. Indeed, the magnitude of this negative shift is directly proportional to the incident photon flux (Figure 9).

Photocharging of semiconductor films and particles has been considered by previous authors.[22] Thus, the use of a Au-plated Pt wire and a Ag/AgCl, saturated KCl reference enabled monitoring of negative potential shifts (of a few millivolts) when the excitation light was turned on.[22] Similarly, use of a pulsed laser revealed a sharp shift in E_{ph} in a negative direction followed by a decay toward the initial potential.[21] This trend is reminiscent of that observed in the present study for the control run and the photocatalytically inert metal ions.

Electron accumulation at the TiO_2/particle surface is followed by trapping events (an analogous scheme can be envisioned for the photogenerated holes, as well). This accounts for the subsequent "relaxation" observed in the ($E-t$) profiles to more positive values (Figures 2 and 4). Therefore, the essential similarity of the profiles for the control run and the presence of photocatalytically inert metal ions may be due to the similar

time course of events in both the instances. Within the framework of this model, and upon ignoring the effects of interfacial charge-transfer kinetics, it is then tempting to associate the plateau potentials attained in these cases to be coincident with the trap state energy location within the TiO_2 band gap. That is, the quasi-Fermi level is ultimately "pinned" to a location where the photogenerated electron−hole pairs undergo trap-mediated recombination. With reference to Figures 1 and 4, these trap states can be located ca. 300−400 mV below the TiO_2 conduction band edge. Further, the data in Figure 8 show that the plateau potential becomes increasingly more positive with decreasing photon flux, diagnosing that a continuum of surface states may exist at energies "deeper" down in the TiO_2 band gap. What is perhaps most surprising in the $E-t$ profiles in Figures 2 and 4 is the significant time span of the relaxation effect—it spans a time domain of the order of minutes!

Examining these data collectively within the framework of results reported by other authors, the following observations are pertinent. Spectroelectrochemical measurements[44] have recorded surface states located at ∼0.5 eV below the conduction band edge. Evidence from a variety of other measurement probes (transient photocurrent,[49] transient absorption,[50] electrolyte electroreflectance,[51] charge recombination kinetics,[52] cyclic voltammetry,[53] ac impedance spectroscopy[54−56]) places the surface trap states at ∼0.5−1.1 eV below the TiO_2 conduction band edge. Our estimate of the trap state location from the data in Figures 2 and 4 is of the same magnitude as literature data. The other aspect concerns the slow rate of the trapping/detrapping events within the nanostructured film. Once again, recent evidence suggests that thermalized electrons (and holes) in irradiated TiO_2 are trapped at the surface and persist as such for minutes.[57] Other studies and discussions underline the rather slow rate of transport of the majority of carriers (electrons) in nanostructured TiO_2 films.[58,59]

While this paper was undergoing peer review, a report appeared[60] on slow surface charge trapping kinetics on UV-irradiated TiO_2 as studied by diffuse reflectance IR spectroscopy. These authors observed that the lifetime of photogenerated electrons can extend several orders of magnitude up to hundreds of minutes.[60] Their IR data were interpreted using trap states located at ∼0.42 eV below the conduction band edge, in rather good agreement with our own estimate (see above).

Our observation, in this study, that metal ions influence the plateau potentials in the ($E_{ph}-t$) profiles, especially when the "depolarizing" influence of the metal ion is weak or absent (Mn^{2+}, Zn^{2+}, Cd^{2+}, Tl^{+}, Pb^{2+}), raises the interesting possibility that interaction of these metal ions with the TiO_2 surface may perturb the trap-state energetics. Once again, we note evidence in the literature for such effects determined by the electrolyte electroreflectance method.[61]

Depolarization of the Photocharged TiO_2/Solution Interface by Electron Acceptors and Donors. It is fruitful to think that the Fermi level (strictly, the quasi-Fermi level) in the irradiated TiO_2 film is "pinned" to the kinetics of the electron-transfer process at the TiO_2/solution interface. That is, facile electron acceptors and donors can "depolarize" the TiO_2 particles (and can short-circuit the electron accumulation at the "photocharged" interface) such that the quasi-Fermi levels in these cases are pinned to very positive and very negative potentials, respectively. These two extreme scenarios are exemplified by the Cr^{6+} and formate cases (Figures 4 and 5). The accumulated charge is depleted by the presence of Cr^{6+} oxidant whereas with formate it is maintained by the reductant. Interestingly, the formate signature is dominant in the $E-t$ profiles even when metal ions are present (Figure 6). This signals that the dominant depolarization event is the initial photooxidation of the co-additive. On the other hand, the relatively mild influence of formate in the presence of Cr^{6+} (Figure 6) can be rationalized on the basis that the co-additive effect is superimposed on an already facile reduction process. Thus formate acts in this case mainly via its influence on the conjugate (photooxidation) reaction pathway and the consequent generation of protons at the interface.[13]

An attempt was made to rationalize the ordering of the co-additive effects discussed earlier with reference to the data in Figure 5, in terms of corresponding variations in the homogeneous reaction cross-sections between these organic species and hydroxyl radicals. A consideration of reported[62] bimolecular rate constants, for the four co-additives studied here, shows that formate does indeed have the highest value for the rate constant (3.2×10^9 L mol^{-1} s^{-1}). However, values for the other three cases are discordant with the formate > oxalate ≫ acetate, methanol trend observed in this study (cf., Figure 5). Thus, other factors (e.g., direct hole transfer, adsorption on the TiO_2 surface) must be operative in the *heterogeneous* reaction environments in our study. Other recent studies, in our laboratory (using point of zero charge measurements), showed that formate and oxalate have a much greater proclivity to binding with the TiO_2 surface relative to acetate and methanol.[63] Further, both formate and oxalate are seen to induce the indirect photocatalytic reduction of Tl^{+} ions in UV-irradiated suspensions in a more facile manner than acetate and methanol.[15] These results are better diagnostics of the causal factors underlying the trends seen in Figure 5 than data on homogeneous reactions.

Finally, the positive shift in the photopotential with decreasing pH in the Cr^{6+} case remains to be accounted for. Our previous studies on this system[13] have shown that a lower pH is beneficial to Cr^{6+} reduction, due to the proton supply needed for this process. In this light, the positive shift can be interpreted in terms of increasing depolarization of the TiO_2 particles by the Cr^{6+} oxidant, as the pH is lowered.

Photon Flux Effects and Discharging of the Photocapacitor. According to our simple photocapacitor model for the TiO_2 film/solution interface, the incident UV light serves to "photocharge" the capacitive interface. Indeed, Figure 9 suggests that a potentiometric photon flux monitor could be set up on the basis of this property of the TiO_2 film. Closer examination of this plot also shows that the parameter ΔE_{ph} does not smoothly go to zero as the photon flux drops to zero. This nonnegligible intercept (168 mV vs Ag/AgCl, saturated KCl) of the plot in Figure 9 (see insert), is diagnostic of an initial rapid increase in the negative potential shift at very low photon fluxes, followed by a linear trend thereafter, as indicated by the subsequent fit of the data points. This "bimodal" behavior of ΔE_{ph} vs photon flux requires further scrutiny.

Given that the parameter ΔE_{ph} may be equated with the (open-circuit) photovoltage (V_{oc}) of photovoltaic systems (such as illuminated semiconductor/liquid and metal/semiconductor junctions), it is pertinent to point out that a plot of ΔE_{ph} versus the logarithm of the light intensity was not linear, as embodied in[64,65]

$$V_{oc} \simeq \frac{nRT}{F} \ln I_L \qquad (1)$$

where I_L is the photon flux, n is the ideality factor, and the other terms have their usual significance. Another way to examine the nonadherence of our photon flux data to the Schottky barrier model[66] represented by eq 1 concerns the

change in V_{oc} for a decade change in the photon flux. For $n = 1$ (ideal rectifier),[66] a decade increase in I_L should translate into a corresponding 60 mV increase in V_{oc} (for $T = 25$ °C). On the other hand, if the transport behavior of the semiconductor/liquid junction is recombination-limited, $n = 2$ and a 120 mV change should result. The changes observed in this study in ΔE_{ph} (Figure 9) are much higher than expected from either of these scenarios.

The above analysis renders additional support for our photocapacitor model of the TiO_2/solution interface rather than an alternate one based on traditional depletion-layer electrostatics. Indeed, we[67] and others[68] have discussed the photoelectrochemical behavior of *nanocrystalline* semiconductor/liquid interfaces in terms of differential charge-transfer kinetics of the photogenerated electrons and holes, rather than in terms of the depletion layer model applicable to *single-crystal* semiconductor cases.[69]

Previous studies using platinized TiO_2 slurries and a Au-plated Pt potential probe have reported[22] that the potential returns to the original value in an exponential manner when the excitation light is turned off. Our new data in Figure 10 (using a different potentiometric configuration) are entirely consistent with this previous result.

Model Simulations. Computer simulations were performed to further support the veracity of our simple photocharging interface model. Thus we designate four steps to be descriptive of the sequence of events upon irradiating the TiO_2 film surface:

a. carrier generation:
$$\left(\frac{d[e^-]}{dt}\right)_g = k_g \quad (2)$$

b. carrier recombination:
$$\left(\frac{d[e^-]}{dt}\right)_r = -k_r[h^+][e^-] \quad (3)$$

c. carrier trapping:
$$\left(\frac{d[e^-]}{dt}\right)_t = -k_t[T][e^-] \quad (4)$$

d. charge transfer:
$$\left(\frac{d[e^-]}{dt}\right)_{ct} = -k_{ct}[OX][e^-] \quad (5)$$

Thus, the net electron accumulation at the surface is given by the rates of (2) − (3) + (4) + (5) above. In the above scheme, the k's are rate constants, T denotes an electron trapping site at the surface, and OX stands for an electron acceptor. The electron and hole concentrations in eqs 2−5 are surface values. We have

$$\frac{d[e^-]}{dt} + \{k_r[h^+] + k_t[T] + k_{ct}[OH]\}[e^-] = k_g \quad (6)$$

If we let the terms inside the brackets to be denoted by a and $k_g = b$, then

$$\frac{d[e^-]}{dt} + a[e^-] = b \quad (7)$$

This differential equation is very easily solved to yield

$$[e^-] = \frac{b}{a}(1 - e^{-at}) \quad (8)$$

With our simple capacitor model ($E = Q/C$, where Q is the charge and C is the interfacial capacitance), we can use eq 8 as the master equation and use a and b as the simulation variables, to generate ($E-t$) profiles. In this first-order exercise, any change in the interfacial capacitance value with time was neglected.

The simulation results in Figure 11 show that our simple model is able to reproduce the essential trends in the experimental ($E-t$) profiles. Thus, Figure 11a is to be compared with the corresponding experimental data in Figure 4 for the control run and experiments involving Zn^{2+}, Cu^{2+}, and Cr^{6+}, respectively. Both the negative excursion, the dependence of its extent on the electron acceptor (or the lack thereof in the control run), and the trends in the plateau potentials are reproduced correctly in these simulations. Similarly, the simulations in Figure 11b pertain to the effect of variable photon flux. Once again, these simulated profiles are to be compared with their counterparts in Figure 8. Thus, the parameter b was maintained constant for the simulations in Figure 11a (because the incident photon flux is constant in the corresponding experiments; see eqs 2, 6, and 7 above), and it was varied in Figure 11b.

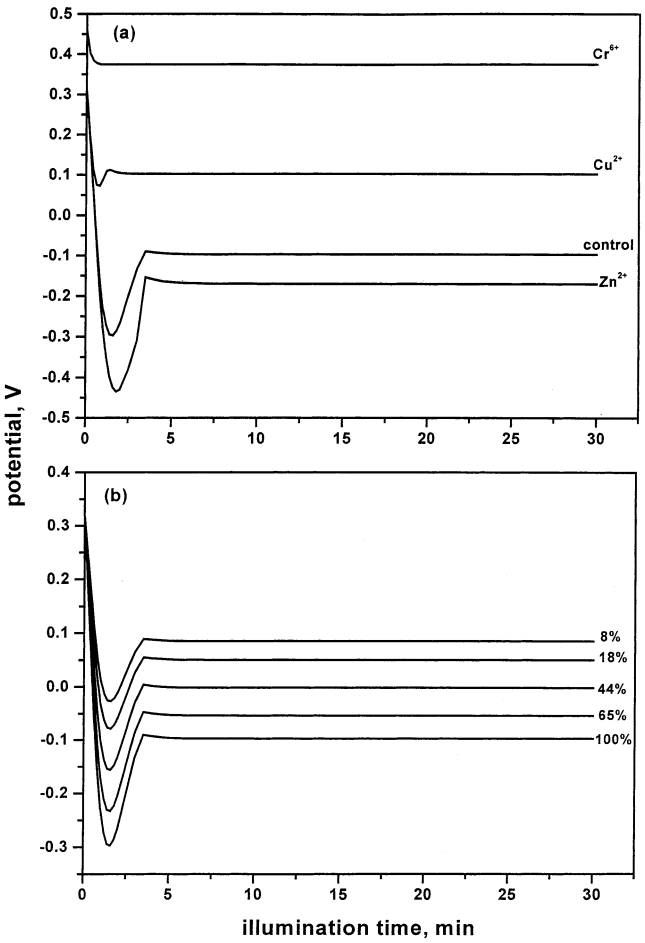

Figure 11. (a) Simulated CP profiles for the control run and three metal ions. The simulation parameters were as follows: Control ($a = 1.15$, $b = 0.48$, offset = 0.32 V), Cr^{6+} ($a = 5.6$, $b = 0.48$, offset = 0.46 V), Cu^{2+} ($a = 2.2$, $b = 0.48$, offset = 0.32 V), and Zn^{2+} ($a = 0.98$, $b = 0.48$, offset = 0.32 V). Experimental counterparts of these profiles in Figure 4. (b) Simulated CP profiles for varying photon fluxes: 100% flux ($a = 1.15$, $b = 0.48$, offset = 0.32 V), 65% ($a = 1.15$, $b = 0.43$, offset = 0.32 V), 44% ($a = 1.15$, $b = 0.37$, offset = 0.32 V), 18% ($a = 1.15$, $b = 0.31$, offset = 0.32 V), and 8% ($a = 1.15$, $b = 0.27$, offset = 0.32 V). Experimental counterparts in Figure 8.

Concluding Remarks

The present study has hopefully illustrated that chronopotentiometry is a useful addition to the arsenal of measurement probes that have been deployed for the study of heterogeneous photocatalytic systems. Our simple model based on photocharging of the TiO_2 film/solution interface by the UV excitation light also appears to be reasonably well borne out by the

computer simulations. The plot in Figure 9 also reveals a possible practical application in the monitoring of photon fluxes. Further variants based on repetitive light on−off cycles and/or the use for light intensity modulations are suggested by the simple, first-order exercise presented in this paper. In this regard, we note that techniques such as intensity-modulated photovoltage spectroscopy have already been developed and applied to a dye-sensitized TiO_2/solution interface by other authors.[70]

Acknowledgment. This research was supported, in part, by a grant from the U.S. Department of Energy, Office of Basic Energy Sciences. We thank a reviewer for constructive criticisms of an earlier version of the manuscript.

References and Notes

(1) Rajeshwar, K.; Ibanez, J. *Environmental Electrochemistry*; Academic Press: San Diego, 1997.
(2) Blake, D. M. Bibliography of Work on the Heterogeneous Photocatalytic Removal of Hazardous Compounds from Water and Air. NREL/TP-570-26797, National Renewable Energy Laboratory, Golden, CO, 1999. Update No. 4 to October 2001, NREL/TP-510-31319. Also see http://www.nrel.gov./chemistrybioenergy/chemistry.html.
(3) Rajeshwar, K. *J. Appl. Electrochem.* **1995**, *25*, 1067.
(4) Litter, M. I. *Appl. Catal. B. Environ.* **1999**, *23*, 89.
(5) Rajeshwar, K.; Ibanez, J. G. *J. Chem. Educ.* **1995**, *72*, 1044.
(6) Gerischer, H.; Heller, A. *J. Phys. Chem.* **1991**, *95*, 5261.
(7) Wang, C.-M.; Heller, A.; Gerischer, H. *J. Am. Chem. Soc.* **1992**, *114*, 5230.
(8) Lin, W.-Y.; Rajeshwar, K. *J. Electrochem. Soc.* **1993**, *140*, 2477.
(9) Lin, W.-Y.; Rajeshwar, K. *J. Electrochem. Soc.* **1997**, *144*, 2751.
(10) Chenthamarakshan, C. R.; Yang, H.; Savage, C. R.; Rajeshwar, K. *Res. Chem. Intermed.* **1999**, *25*, 861.
(11) Chenthamarakshan, C. R.; Rajeshwar, K. *Electrochem. Commun.* **2000**, *2*, 527.
(12) Chenthamarakshan, C. R.; Yang, H.; Ming, Y.; Rajeshwar, K. *J. Electroanal. Chem.* **2000**, *494*, 79.
(13) Chenthamarakshan, C. R.; Rajeshwar, K.; Wolfrum, E. J. *Langmuir* **2000**, *16*, 2715.
(14) Goeringer, S.; Chenthamarakshan, C. R.; Rajeshwar, K. *Electrochem. Commun.* **2001**, *3*, 290.
(15) Kajitvichyanukul, P.; Chenthamarakshan, C. R.; Rajeshwar, K.; Qasim, S. R. *J. Electroanal. Chem.* **2002**, *519*, 25.
(16) Ming, Y.; Chenthamarakshan, C. R.; Rajeshwar, K. *J. Photochem. Photobiol. A: Chem.* **2002**, *147*, 199.
(17) Rajeshwar, K.; Chenthamarakshan, C. R.; Goeringer, S.; Djukic, M. *Pure Appl. Chem.* **2001**, *73*, 1849.
(18) Rajeshwar, K.; Chenthamarakshan, C. R.; Ming, Y.; Sun, W. *J. Electroanal. Chem.*, in press.
(19) Bard, A. J.; Faulkner, L. R. *Electrochemical Methods*; J. Wiley: New York, 1980; Chapter 7, p 249.
(20) Of course, there is no *net* current flow across the working electrode/solution interface in the potentiometric measurements reported here.
(21) Perone, S. P.; Richardson, J. H.; Deutscher, S. B.; Rosenthal, J.; Ziemer, J. N. *J. Electrochem. Soc.* **1980**, *127*, 2580.
(22) Uosaki, K.; Kita, H. *J. Electrochem. Soc.* **1982**, *129*, 1752.
(23) Separate control runs using uncoated Au electrodes showed that $E_{ph}-t$ profiles of the sort shown in Figures 2 and 4-6 cannot be attributed to the underlying gold surface.
(24) The simple metal ion designation used here does not take speciation into account. For example, the notation "Cr^{6+}" is employed for descriptive convenience although the dominant hexavalent chromium species (at the pHs of relevance here) are the dichromate oxyanions. Further, complexation of the metal ions is not expected to play an appreciable role in the data presented (especially in the absence of the organic co-additives) because the pH was not intentionally varied except in the experiments considered in Figures 3 and 7.
(25) Yates, D. E.; Levine, S.; Healy, T. W. *J. Chem. Soc., Faraday Trans. 1* **1974**, *70*, 1807.
(26) Davis, J. A.; Leckie, J. O. *J. Colloid Interface Sci.* **1980**, *74*, 32.
(27) Morrison, S. R. *Electrochemistry of Semiconductor and Oxidized Metal Electrodes*; Plenum: New York, 1980.
(28) Pleskov, Yu. V.; Gurevich, Yu. Ya. *Semiconductor Photoelectrochemistry*; Consultants Bureau (Plenum): New York and London, 1986.
(29) Dutoit, E. C.; Cardon, F.; Gomes, W. P. *Ber. Bunsen-Ges. Phys. Chem.* **1976**, *80*, 475.
(30) Fitzmaurice, D. *Solar Energy Mater. Solar Cells* **1994**, *32*, 289.
(31) Borgarello, E.; Kiwi, J.; Pelizzetti, E.; Visca, M.; Grätzel, M. *J. Am. Chem. Soc.* **1981**, *103*, 6324.
(32) Grätzel, M.; Frank, A. J. *J. Phys. Chem.* **1982**, *86*, 2964.
(33) Avena, M. J.; Camara, O. R.; de Pauli, C. P. *Colloids Surf.* **1993**, *69*, 217.
(34) Duonghang, D.; Borgarello, E.; Grätzel, M. *J. Am. Chem. Soc.* **1981**, *103*, 4685.
(35) Kolle, U.; Moser, J.; Grätzel, M. *Inorg. Chem.* **1985**, *24*, 2253.
(36) Rothenberger, G.; Moser, J.; Grätzel, M.; Serpone, N.; Sharma, D. K. *J. Am. Chem. Soc.* **1985**, *107*, 8054.
(37) Furuke, A.; Asahi, T.; Masuhara, H.; Yamashita, H.; Anpo, M. *J. Phys. Chem. B* **1999**, *103*, 3120.
(38) Howe, R. F.; Grätzel, M. *J. Phys. Chem.* **1985**, *89*, 4495.
(39) Moser, J.; Punchihewa, S.; Infelta, P.; Grätzel, M. *Langmuir* **1991**, *7*, 3012.
(40) Dloczik, L.; Ileperuma, O.; Lauermann, I.; Peter, L. M.; Ponomarev, E. A.; Redmond, G.; Shaw, N. J.; Uhlendorf, I. *J. Phys. Chem. B* **1997**, *101*, 10281.
(41) Mandelbaum, P. A.; Regazzoni, A. E.; Blesa, M. A.; Bilmes, S. A. *J. Phys. Chem. B* **1999**, *103*, 5505.
(42) Solbrand, A.; Henningsson, A.; Södergren, S.; Lindstrom, H.; Hagfeldt, A.; Lindquist, S.-E. *J. Phys. Chem. B* **1999**, *103*, 1078.
(43) Park, N.-G.; Schlichthorl, G.; van de Lagemaat, J.; Cheong, H. M.; Mascarenhas, A.; Frank, A. J. *J. Phys. Chem. B* **1999**, *103*, 3308.
(44) Boschloo, G.; Fitzmaurice, D. *J. Phys. Chem. B* **1999**, *103*, 2228.
(45) Rajh, T.; Nedeljkovic, J. M.; Chen, L. X.; Poluektov, O.; Thurnauer, M. C. *J. Phys. Chem. B* **1999**, *103*, 3515.
(46) Lemon, B. I.; Hupp, J. T. *J. Phys. Chem. B* **1999**, *103*, 3797.
(47) Vanmaekelbergh, D.; de Jongh, P. E. *J. Phys. Chem. B* **1999**, *103*, 747.
(48) Lyon, L. A.; Hupp, J. T. *J. Phys. Chem. B* **1999**, *103*, 4623.
(49) Boschloo, G. K.; Goossens, A. *J. Phys. Chem.* **1996**, *100*, 19489.
(50) Redmond, G.; Grätzel, M.; Fitzmaurice, D. *J. Phys. Chem.* **1993**, *97*, 6951.
(51) Boschloo, G. K.; Goossens, A.; Schoonman, J. *J. Electroanal. Chem.* **1997**, *428*, 25.
(52) Haque, S. A.; Tachibana, Y.; Klug, D. R.; Durrant, J. R. *J. Phys. Chem. B* **1998**, *102*, 1745.
(53) Kavan, L.; Kratochvilova, K.; Grätzel, M. *J. Electroanal. Chem.* **1995**, *394*, 93.
(54) Tomkiewicz, M. *J. Electrochem. Soc.* **1980**, *127*, 1518.
(55) Siripala, W.; Tomkiewicz, M. *J. Electrochem. Soc.* **1981**, *128*, 2491.
(56) Siripala, W.; Tomkiewicz, M. *J. Electrochem. Soc.* **1982**, *129*, 1240.
(57) Grela, M. A.; Colussi, A. J. *J. Phys. Chem. B* **1999**, *103*, 2614.
(58) Kelly, J. J.; Vanmaekelbergh, D. *Electrochim. Acta* **1998**, *43*, 2773.
(59) Hagfeldt, A.; Grätzel, M. *Chem. Rev.* **1995**, *95*, 49.
(60) Szczepankiewicz, S. H.; Moss, J. A.; Hoffmann, M. R. *J. Phys. Chem. B* **2002**, *106*, 2922.
(61) Poznyak, S. K.; Pergushov, V. I.; Kokorin, A. I.; Kulak, A. I.; Schälpfer, C. W. *J. Phys. Chem. B* **1999**, *103*, 1308.
(62) Buxton, G. V.; Greenstock, C. L.; Helman, W. P.; Ross, A. B. *J. Phys. Chem. Ref. Data* **1988**, *17*, 513.
(63) Kajitvichyanukul, P.; Chenthamarakshan, C. R.; Rajeshwar, K.; Qasim, S. R. To be submitted.
(64) Rajeshwar, K.; Thompson, L.; Singh, P.; Kainthla, R. C.; Chopra, K. L. *J. Electrochem. Soc.* **1981**, *128*, 1744.
(65) Lewis, N. S. *J. Electrochem. Soc.* **1984**, *131*, 2496.
(66) Rhoderick, E. H. *Metal − Semiconductor Contacts*; Clarendon Press: Oxford, U.K., 1980.
(67) de Tacconi, N. R.; Carmona, J.; Rajeshwar, K. *J. Phys. Chem. B* **1997**, *101*, 10151.
(68) Hodes, G.; Howell, I. D.; Peter, L. M. *J. Electrochem. Soc.* **1992**, *139*, 3136.
(69) Rajeshwar, K. In *Electron Transfer in Chemistry*; Balzani, V., Ed.; Wiley-VCH: Weinhem, 2001.
(70) Frank, A. J. Personal communication (to K.R.), 2001.